Hindawi
Journal of Nanomaterials
Volume 2020, Article ID 8725390, 8 pages
https://doi.org/10.1155/2020/8725390

Research Article

Study on the Thermal Conductivity of Mannitol Enhanced by Graphene Nanoparticles for Thermoelectric Power Generation

Jia Yu, Haoqing Wang, Li Kong, Hongji Zhu, and Qingshan Zhu

College of Aerospace and Civil Engineering, Harbin Engineering University, Harbin 150001, China

Correspondence should be addressed to Jia Yu; yujiaworld@163.com and Haoqing Wang; freedom1322@163.com

Received 19 January 2020; Revised 15 June 2020; Accepted 27 July 2020; Published 17 October 2020

Academic Editor: Yasuhiko Hayashi

The existing thermoelectric materials are greatly affected by the temperature environment, which can provide better power output in a stable temperature environment by using composite phase change material with enhanced heat conduction. The graphene is dispersed in the liquid mannitol to make the nanomixed material. Test results show that the thermal conductivity of mannitol increased from 0.7 $Wm^{-1}K^{-1}$ to 2.07 $Wm^{-1}K^{-1}$, 179.73% times as much. The effective thermal conductivity of mannitol can be increased to 8.4236 $Wm^{-1}K^{-1}$ by using a graphite foam with a porosity of 0.9. After adding 1 wt.% and 5 wt.% graphene particles, the effective thermal conductivity increased to 8.73 $Wm^{-1}K^{-1}$ and 9.63 $Wm^{-1}K^{-1}$, respectively. The simulation results in a large heat source environment show that mannitol with improved thermal conductivity can ensure the stable operation of the thermoelectric material in the optimal temperature environment for 120 s, and the open-circuit voltage is maintained at about 6.5 V in that time.

1. Introduction

Phase change materials (PCMs) control the temperature of the surrounding environment by absorbing or releasing its latent heat in the process of phase change [1]. They are applied and studied in aerospace, electronic equipment, solar power generation, and other fields [2, 3]. However, most PCMs have the disadvantage of low thermal conductivity, such as paraffin [4] and salt [5]. The low heat transfer rate has a great impact on the heat transfer process, so it is very important to improve the thermal conductivity of PCMs. The common methods to enhance heat transfer are using fin structure [6], using capsule structure [7, 8], using porous medium structure [9, 10], and adding high thermal conductivity material [11, 12]. Two or more methods can be used to further improve the thermal conductivity, such as mixing paraffin wax with expanded graphite and then adding the nanomixed material to the aluminum foam [13, 14]. Zhao et al. added fins to a two-dimensional heat exchange tube model and studies the influence of fin position. Their results show that adding fins can reduce the melting time by 12%, but the influence of fin position is small, and the fin position can be adjusted to reduce other design difficulties [15]. Do et al. designed a capsule structure of phase change material which could improve the efficiency of energy absorption or release by 41%, but the capsule was easy to be damaged [16]. Chunhui et al. developed a phase change material thermal storage unit made by aluminum foam and nitrogen. Their test result shows that the maximum temperature difference between the up and bottom of the thermal storage unit is less than 0.5 K, much lower than the case without aluminum foam [17]. Marcos et al. used graphene nanoplatelets to enhance the thermal conductivity and the nanoenhanced phase change materials could reach 23% for 0.50% fGnP/PEG 400 nanofluid, while ensuring small changes in other thermal properties [18].

Thermoelectric material is a kind of clean energy, which can directly generate electric energy through temperature gradient. Temperature directly affects the performance of thermoelectric conversion, such as the maximum temperature range, temperature difference between two sides of thermoelectric material, and temperature distribution between multistage materials [19, 20]. PCMs can provide a stable power generation environment for thermoelectric materials

[21, 22]. The research of this kind of power generation structure has appeared, such as high-temperature power generation on aircraft, power supply of underwater glider [23], and airborne sensor [24, 25]. PCMs can be used on the hot side of thermoelectric power generation (TEG) to reduce the temperature change [26], and it is necessary to improve the thermal conductivity of PCMs [27, 28].

The commercial TEG-126T200 is purchased in our laboratory. Considering the maximum temperature that the TEG can bear is about 200°C, mannitol with a melting point of 167°C is selected as PCMs. This paper is aimed at further improving the thermal conductivity of graphite foam composites by using graphene nanomaterials because using graphite foam has a certain limit. Experiments and simulation are both used in this paper.

2. Experimental Section

2.1. Preparation of Materials. In order to compare and observe the effect of graphene, several groups of experimental materials were prepared, and the preparation process is shown in Figure 1. The nanomaterials of the specified quality are filled into the liquid mannitol. The mixed liquid with good dispersity is obtained by using a magnetic stirrer and ultrasonic wave for 3 hours. Part of the mixed liquid is selected to stand in the vacuum drying oven until it is cooled to room temperature to obtain nanomixed materials. As seen in Figure 2(a), graphite foams with porosity of 0.9 are cut into about $40 * 40 * 20\ mm^3$ of size and mixed with the last part of the mixed liquid, and then the final composite PCMs were prepared by the same cooling method. In Figure 2(b), we can see the obvious graphene lamellar structure. The in-plane thermal conductivity of graphene is very high, but the thermal conductivity between different layers is low. The size of this lamellar structure is the reference for the following modeling.

In Figure 2(c), the skeleton of graphite foam can be observed. It can be seen that the interface between graphite foams and mannitol is clear and filled with fullness. The mannitol is completely coated on the graphite skeleton, which indicates that the nanomodified mannitol can meet the requirements of filled carbon foams. Figure 2(d) is the dispersion of graphite foam in mannitol. In the photos, we can see the obvious graphene lamellar structure. The graphene overlaps with each other in mannitol, thus forming a connected heat transfer channel, which will help to improve the thermal conductivity of the composite material.

2.2. Test Data of Nanomaterials. Figure 3 shows the test results of the above materials after repeated melting. It can be seen that both pure mannitol and graphene-mannitol are stable, and the DSC curve has not changed significantly after 50 times of repeated heating, indicating that the material can be reused in practice. On the other hand, due to the addition of graphene, the thermal conductivity of mannitol has been improved, and the maximum heat flow peak value can be obviously reduced in the figure. The reduction of the maximum heat flow peak value in Figure 3 is a direct reflection of the improvement of the thermal conductivity of the composite. Because in the same heating process, the larger thermal conductivity can make the heat transfer to the whole sample quickly, so the maximum peak value decreases and the transverse area becomes wider obviously.

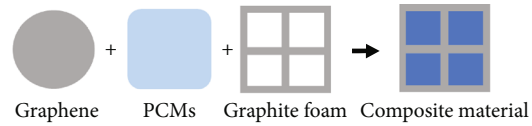

Figure 1: Schematic diagram of the composite material preparation process.

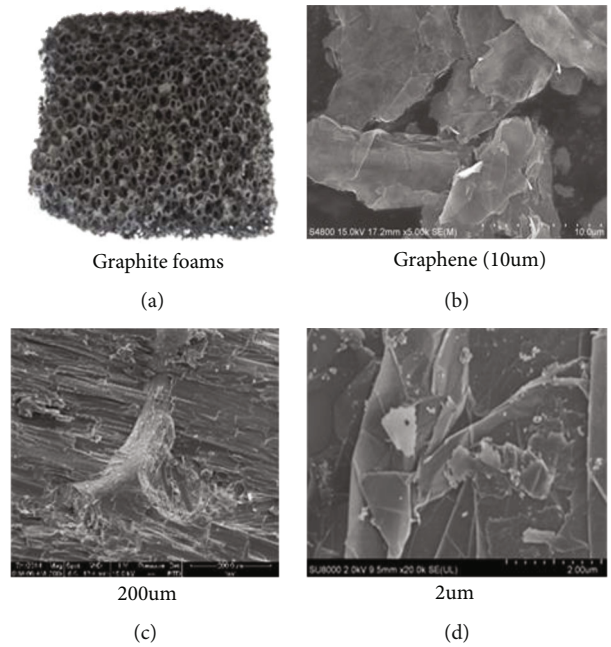

Figure 2: Image of graphite foam, graphene, and composite materials.

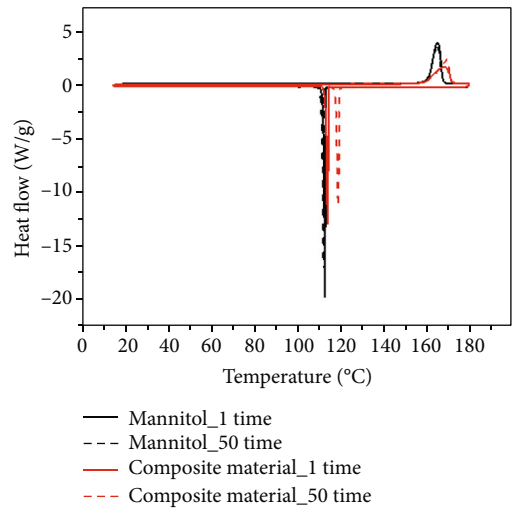

Figure 3: Comparison of the effects of heating cycles.

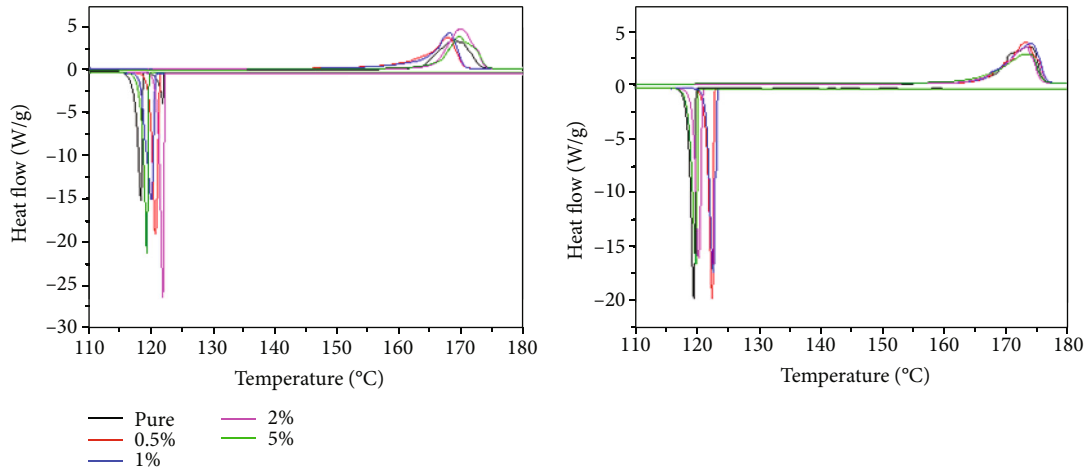

Figure 4: DSC curve of graphene-mannitol sample (a) and graphene-mannitol-foams (b).

Table 1: DSC test data of graphene-mannitol sample.

Ratio	Liquidus point (°C)	Liquidus heat ($kJkg^{-1}$)	Solidus point (°C)	Solidus heat ($kJkg^{-1}$)
0 wt.%	165.3	307.4	118.4	266.8
0.5 wt.%	164.6	305.8	121.6	259.6
1 wt.%	165.8	304.6	120.8	256.8
2 wt.%	166.6	299.0	119.5	254.3
5 wt.%	165.0	288.3	120.6	252.2

Table 2: DSC test data of graphene-mannitol-foam sample.

Ratio	Liquidus point (°C)	Liquidus heat ($kJkg^{-1}$)	Solidus point (°C)	Solidus heat ($kJkg^{-1}$)
0 wt.%	169.4	254.1	119.8	217.7
0.5 wt.%	168.2	255.2	122.7	221.5
1 wt.%	166.4	250.9	123.0	217.9
2 wt.%	167.6	245.7	120.8	228.5
5 wt.%	166.7	235.5	120.1	203.0

Figure 4 shows the test results of composite materials with different mass fractions. It can be seen that the DSC curve trend of the composite is basically the same as that of the pure phase change material, and there is no other heat absorption or exothermic peak. This indicates that graphene and graphite foams are only a simple physical combination with mannitol. However, because of the existence of graphene, the latent heat of phase transition of the composite is lower than that of pure mannitol, which can be seen from Tables 1 and 2.

Graphene is a kind of lamellar structure with a thickness of only 0.4-8 nm and a radial direction of up to 2-3 μm. Because of the great difference between the radial direction and the thickness direction, it is easy to form a local or even global heat conduction path when dispersed in phase change materials, so as to improve the thermal conductivity. Figure 5

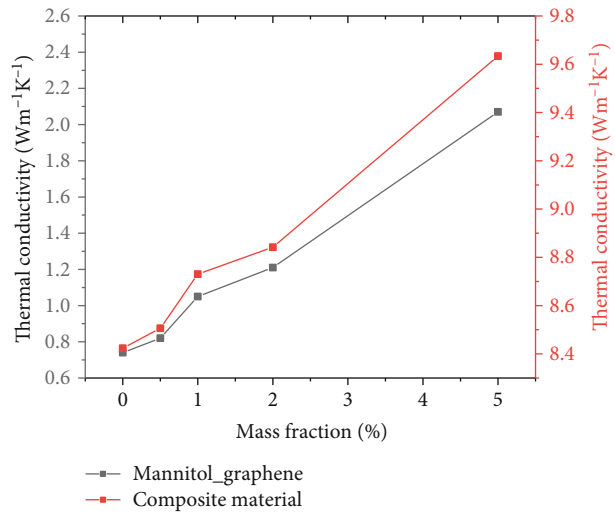

Figure 5: Test data of thermal conductivity.

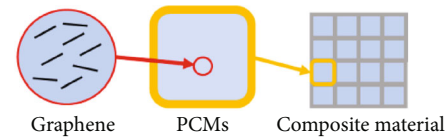

Figure 6: Schematic diagram of simulation model of composite material.

shows the test results of thermal conductivity. It can be seen that the thermal conductivity of mannitol can be increased from 0.74 $Wm^{-1}K^{-1}$ to 8.42 $Wm^{-1}K^{-1}$ by using graphite foam. On the other hand, graphene can further enhance the thermal conductivity. When the graphite foam is not used, the thermal conductivity of mannitol can be increased to 2.07 $Wm^{-1}K^{-1}$, and it can be increased to 9.63 $Wm^{-1}K^{-1}$ after using graphite foam. Therefore, it is feasible to use graphene to further improve the thermal conductivity when the graphite foam reaches its limit.

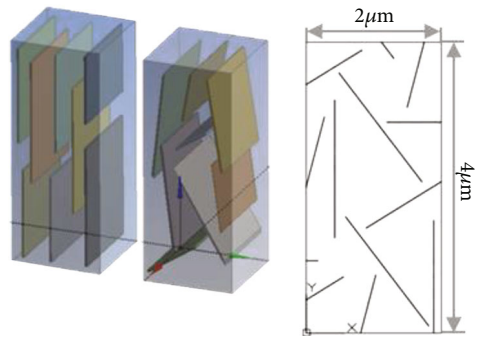

Figure 7: Schematic diagram of graphene lamellar model.

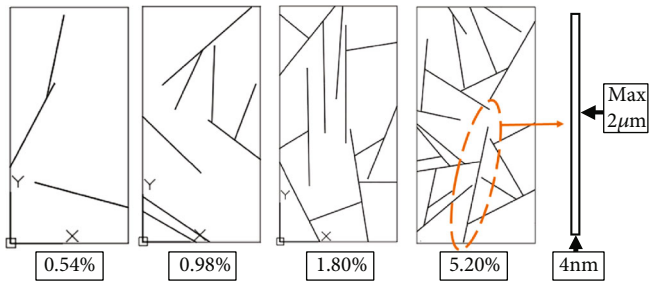

Figure 8: Modeling results of graphene with different mass fraction.

3. Simulation and Discussion

3.1. Simulation of Heat Transfer Process at Different Scales. The addition of graphene with different mass fraction in the phase change material will lead to the change of the effective thermal conductivity of the composite. The thermal conductivity of graphene can be studied by molecular dynamic simulation [29]. In order to directly observe the influence of graphene material on the heat transfer process, this paper conducts simulation calculation at different scales, and the setting of the calculation model is shown in Figure 6. The thermal conductivities of mannitol, graphene, and graphite foam were set at 0.74 $Wm^{-1}K^{-1}$, 1500 $Wm^{-1}K^{-1}$, and 418.18 $Wm^{-1}K^{-1}$, respectively.

Firstly, the graphene is analyzed. On the left side of Figure 7(a) is an idealized graphene distribution model, whose distribution pattern is regular, but it is more complicated in practice just like the model on the right side. Graphite foam is a thin layer structure. There may be physical contact between multiple graphene layers, but no crossover occurs. As shown in Figure 7(b), the distribution model of graphene is established in the two-dimensional XY coordinate system. The coordinates of the center point and the tilt angle of each graphene sheet are generated by using the random function in MATLAB software, and the basic requirements of no crossover in the modeling are met by trimming operation. The initial thickness of graphene is set as 4 nm, and the initial length is 2 μm. The operation of drawing repeatedly until the scale requirements are met. After calculation, it can be considered that the mass fraction of graphene in the model is twice of the volume fraction, that is to say,

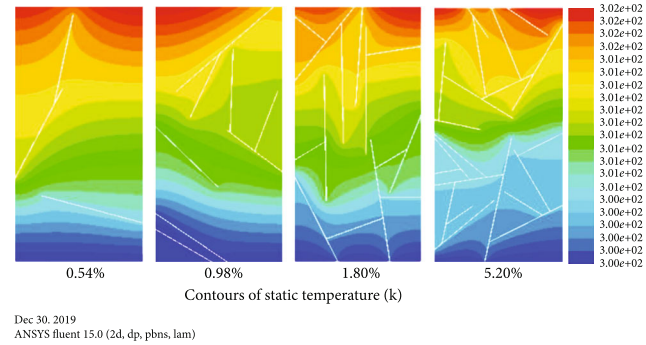

Figure 9: Calculation results of temperature at different volume fraction.

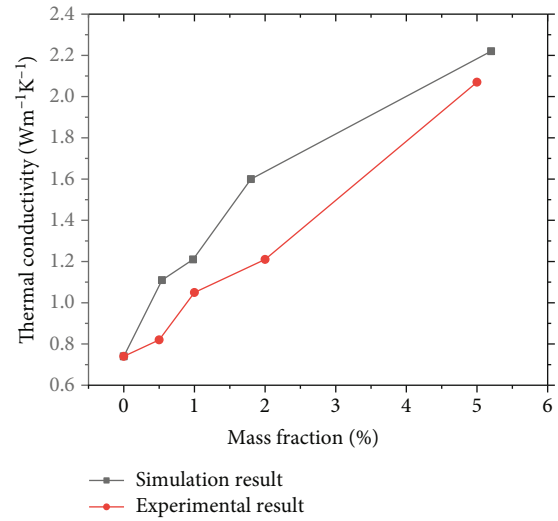

Figure 10: Comparison of thermal conductivity between calculation and experimental results.

every 1 wt.% of graphene is equal to about 0.5% of the total volume. By setting a constant temperature difference at the upper and lower ends of the two-dimensional model, the effective thermal conductivity of the composite can be calculated by the Fourier heat transfer formula. The modeling results are shown in Figure 8.

The thermal conductivity can be calculated in FLUENT. It can be seen from Figure 9 that graphene sheets form a thermal path, and the effective thermal conductivity increases with the increase of graphene sheet content, which is consistent with the trend of experimental results. Obviously, along the heat transfer direction of graphene, the temperature gradient is small, and with the increase of heat transfer channel, the thermal conductivity is higher. As seen in Figure 10, the thermal conductivity of 1 wt.% and 5 wt.% is 1.21 $Wm^{-1}K^{-1}$ and 2.22 $Wm^{-1}K^{-1}$, respectively, which are 17.5% and 12.1% higher than the experimental results. The main reason is that the interface thermal resistance is not considered in the simulation calculation. Therefore, it can be concluded that if the interface thermal resistance between graphene and PCMs can be reduced, the thermal conductivity of the PCMs can be further improved.

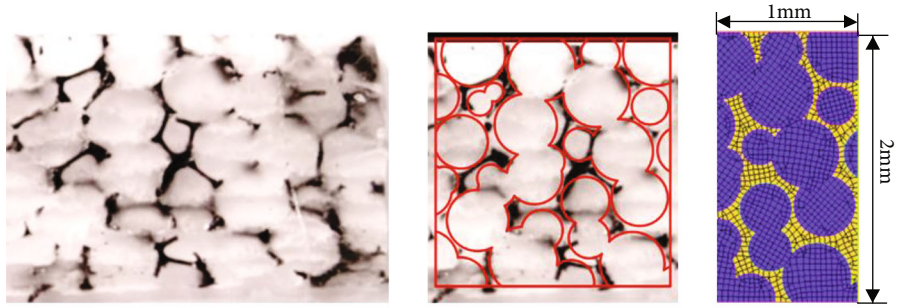

Figure 11: Modeling process of graphite foam.

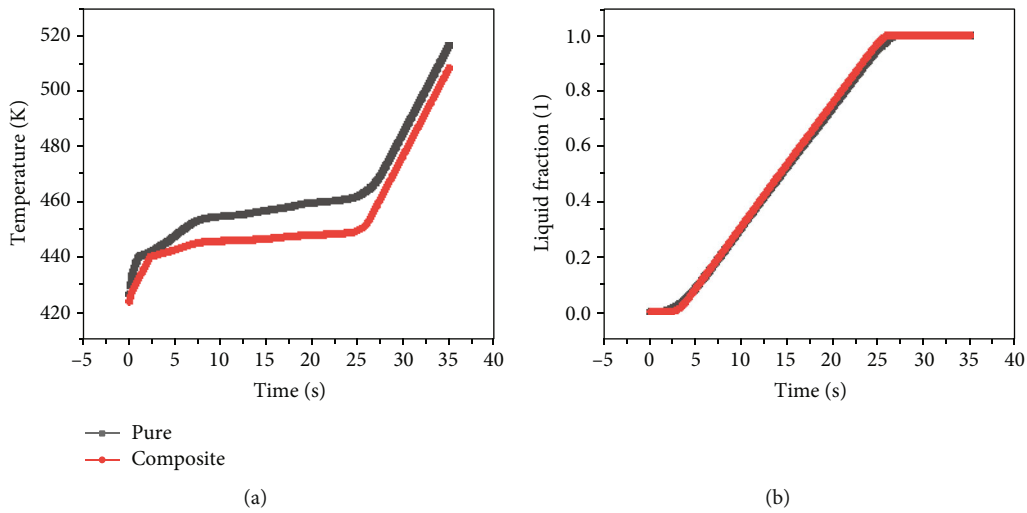

Figure 12: Calculation results of different materials.

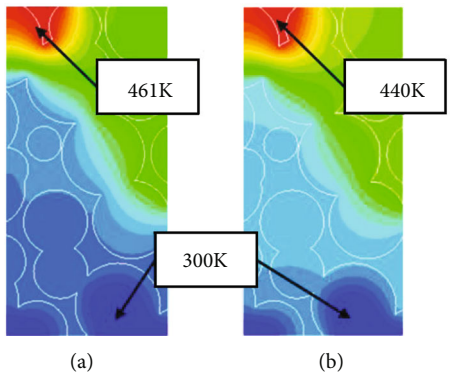

Figure 13: Comparison between pure mannitol (a) and composite material (b).

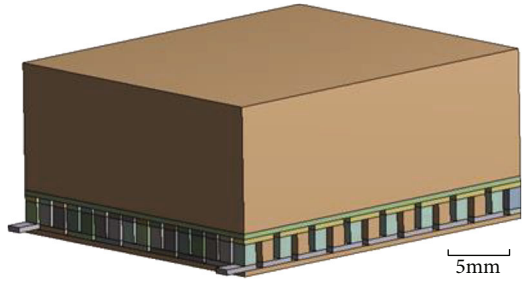

Figure 14: Simulation model of composite material and TEG.

In order to observe the effect of graphene on heat transfer from the scale of graphite foam, a more accurate result can be obtained by using the model close to the actual foam structure in calculation [30]. Considering the cost problem, in this paper, the modeling method is to use a circle in CAD software to simulate the distribution of phase change materials, as shown in Figure 11. It is too difficult to model the graphite foam and graphene according to the actual size. Therefore, graphene and mannitol are regarded as a new material, and their parameters are set according to the ratio. The heat flow condition is 100 kWm^{-2}. The size of the model is $2 * 1\ mm^2$, with the largest pore diameter of graphite foam is 400 μm, and the mass fraction of graphene is 5 wt.%.

It can be seen from Figure 12(a) that the temperature control ability of mannitol is strengthened after the addition of graphene material. On the one hand, the temperature control temperature range is more stable. Graphene composite can maintain the temperature near the melting point, and its maximum temperature is very close to the 440 k melting point. The maximum temperature of complete melting is only about 9.6 K higher than the melting point. When using pure mannitol, the highest temperature is around 460 k,

Table 3: Material parameters.

Material	Density (kgm^{-3})	Specific heat ($kJkg^{-1}K^{-1}$)	Thermal conductivity ($Wm^{-1}K^{-1}$)	Latent heat ($kJkg^{-1}$)	Melting point (K)
Mannitol	1.521	2000	0.74	316.4	167.59
TEG	7740	152	1.5	/	/

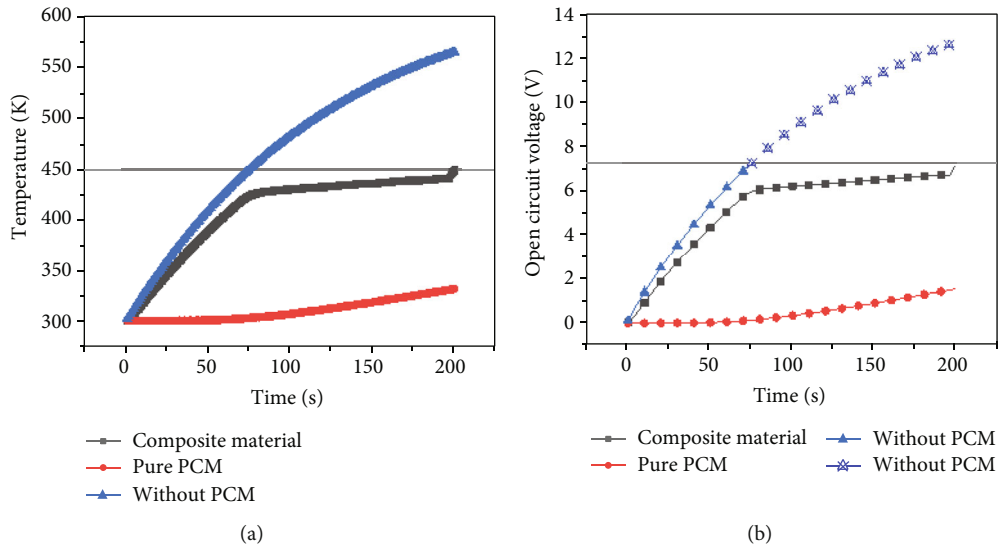

Figure 15: (a) Temperature curve of TEG hot side and (b) liquid fraction curve.

which is about 20 K higher than the melting point. On the other hand, the increase of thermal conductivity makes the heat transfer in the whole structure quickly. It can be seen from Figure 13 that the temperature gradient of pure material on the heat transfer path is large, but after adding graphene, the temperature gradient decreases and the temperature distribution is more uniform. Therefore, in Figure 12(b), the composite material starts to melt later and reaches the state of complete melting earlier.

3.2. Simulation of Temperature Control and Power Generation Structure. It is feasible to use phase change materials to control the temperature of thermoelectric materials. Graphene composite phase change materials with a porosity of 0.9 and a mass fraction of 5 wt.% are calculated in this paper. The calculation model is shown in Figure 14. In the calculation, the heat source is 100 kWm^{-2} and the convection heat transfer coefficient at the cold end is 1500 $Wm^{-2}K^{-1}$, and the environmental temperature is 300 K. In order to simplify the calculation process, TEG is regarded as an entity for calculation, and its parameter setting can refer to the data [28] in the literature, as shown in Table 3.

The calculation results are shown in Figure 15. It can be seen that the composite material can provide a very suitable power generation environment for thermoelectric materials. When the phase change material is not used, the temperature at the hot end of TEG is over 473.15 K too early, the temperature difference between the two ends of thermoelectric materials is very large, resulting in high electricity. But as mentioned before, the maximum temperature that TEG can withstand is about 200°C, thus this case may cause damage to the thermoelectric material. However, when the pure phase change material is used, due to the low thermal conductivity, the heat is not transferred to the hot end of TEG in time, and the electric energy generated is too small.

Obviously, mannitol with improved thermal conductivity is the best solution. In this case, the thermoelectric material can rapidly heat up to obtain a large temperature difference and maintain the temperature stable between 440-450 K for 120 s, and the open-circuit voltage generated by TEG is also stable at about 6.5 V.

4. Conclusions

In this paper, high thermal conductivity composite phase change materials were prepared by graphene nanomaterials, graphite foam, and phase change materials. On the basis of graphite foam, the thermal conductivity of mannitol can be increased from 0.74 $Wm^{-1}K^{-1}$ to 9.65 $Wm^{-1}K^{-1}$ by using graphene nanomaterials. Through the simulation calculation, under the heat source of 100 kWm^{-2}, using mannitol composite material can maintain a stable temperature difference of 120 s. During this period of time, the thermoelectric material can generate an open circuit voltage of 6.5 V and will not be damaged by high temperature. It can be concluded that it is feasible to use the PCMs strengthened by the graphene nanomaterial as the thermal control structure of TEG in high-temperature environment.

Data Availability

All data included in this study are available upon request by contact with the corresponding author.

Conflicts of Interest

The authors declare no competing financial interest.

Acknowledgments

We gratefully acknowledge the financial support of this study by the National Natural Science Foundation of China (Project No. 51672054).

References

[1] Z. Khan, Z. Khan, and A. Ghafoor, "A review of performance enhancement of PCM based latent heat storage system within the context of materials, thermal stability and compatibility," *Energy Conversion and Management*, vol. 115, pp. 132–158, 2016.

[2] W. F. Wu, N. Liu, W. L. Cheng, and Y. Liu, "Study on the effect of shape-stabilized phase change materials on spacecraft thermal control in extreme thermal environment," *Energy Conversion and Management*, vol. 69, pp. 174–180, 2013.

[3] Y. Zhang, G. G. Gurzadyan, M. M. Umair et al., "Ultrafast and efficient photothermal conversion for sunlight-driven thermal-electric system," *Chemical Engineering Journal*, vol. 344, pp. 402–409, 2018.

[4] Y. Hao, X. Shao, and H. Tang, "Preparation and properties of paraffin/TiO2/active- carbon composite phase change materials," *Cailiao Gongcheng/Journal of Materials Engineering*, vol. 44, no. 11, pp. 51–55, 2016.

[5] X. Zhang, X. Li, Y. Zhou et al., "Enhanced thermal conductivity in a hydrated salt PCM system with reduced graphene oxide aqueous dispersion," *RSC Advances*, vol. 8, no. 2, pp. 1022–1029, 2018.

[6] M. Augspurger, K. K. Choi, and H. S. Udaykumar, "Optimizing fin design for a PCM-based thermal storage device using dynamic Kriging," *International Journal of Heat and Mass Transfer*, vol. 121, pp. 290–308, 2018.

[7] X. Wang, Y. Guo, J. Su, X. Zhang, N. Han, and X. Wang, "Microstructure and thermal reliability of microcapsules containing phase change material with self-assembled graphene/organic nano-hybrid shells," *Nanomaterials*, vol. 8, no. 6, p. 364, 2018.

[8] P. A. Advincula, A. C. de Leon, B. J. Rodier, J. Kwon, R. C. Advincula, and E. B. Pentzer, "Accommodating volume change and imparting thermal conductivity by encapsulation of phase change materials in carbon nanoparticles," *Journal of Materials Chemistry A*, vol. 6, no. 6, pp. 2461–2467, 2018.

[9] Y. Li, J. Li, Y. Deng, W. Guan, X. Wang, and T. Qian, "Preparation of paraffin/porous TiO_2 foams with enhanced thermal conductivity as PCM, by covering the TiO_2 surface with a carbon layer," *Applied Energy*, vol. 171, pp. 37–45, 2016.

[10] S. Ye, Q. Zhang, D. Hu, and J. Feng, "Core–shell-like structured graphene aerogel encapsulating paraffin: shape-stable phase change material for thermal energy storage," *Journal of Materials Chemistry A*, vol. 3, no. 7, pp. 4018–4025, 2015.

[11] G. Qiao, M. Lasfargues, A. Alexiadis, and Y. Ding, "Simulation and experimental study of the specific heat capacity of molten salt based nanofluids," *Applied Thermal Engineering*, vol. 111, pp. 1517–1522, 2017.

[12] T.-P. Teng, S.-P. Yu, T.-C. Hsiao, and C.-C. Chung, "Study on the phase change characteristics of carbon-based nanofluids," *Journal of Nanomaterials*, vol. 2018, Article ID 8230120, 12 pages, 2018.

[13] J. Ruiz, Y. Ganatra, A. Bruce, J. Howarter, and A. M. Marconnet, "Investigation of aluminum foams and graphite fillers for improving the thermal conductivity of paraffin wax-based phase change materials," in *2017 16th IEEE Intersociety Conference on Thermal and Thermomechanical Phenomena in Electronic Systems (ITherm)*, pp. 384–389, Orlando, FL, USA, 2017.

[14] Z. Yin, X. Zhang, Z. Huang et al., "Paraffin/expanded graphite phase change composites with enhanced thermal conductivity prepared by implantedβ-SiC nanowires with chemical vapor deposition method," *Materials Research Express*, vol. 5, no. 2, 2018.

[15] L. Zhao, Y. Xing, X. Liu, and Z. Rui, "Heat transfer enhancement in triplex-tube latent thermal energy storage system with selected arrangements of fins," *IOP Conference Series: Earth and Environmental Science*, vol. 108, article 052018, 2018.

[16] T. Do, Y. G. Ko, Y. Jung, and U. S. Choi, "Highly durable and thermally conductive shell-coated phase-change capsule as a thermal energy battery," *ACS Applied Materials & Interfaces*, vol. 12, no. 5, pp. 5759–5766, 2020.

[17] K. Chunhui, C. Liubiao, W. Xianlin, Z. Yuan, and W. Junjie, "Thermal conductivity of open cell aluminum foam and its application as advanced thermal storage unit at low temperature," *Rare Metal Materials and Engineering*, vol. 47, no. 4, pp. 1049–1053, 2018.

[18] M. A. Marcos, D. Cabaleiro, M. J. G. Guimarey et al., "PEG 400-based phase change materials nano-enhanced with functionalized graphene nanoplatelets," *Nanomaterials*, vol. 8, no. 1, p. 16, 2018.

[19] M. Jaworski, M. Bednarczyk, and M. Czachor, "Experimental investigation of thermoelectric generator (TEG) with PCM module," *Applied Thermal Engineering*, vol. 96, pp. 527–533, 2016.

[20] Y. Wu, J. Yang, S. Chen, and L. Zuo, "Thermo-element geometry optimization for high thermoelectric efficiency," *Energy*, vol. 147, pp. 672–680, 2018.

[21] M. E. Kiziroglou, S. W. Wright, T. T. Toh, P. D. Mitcheson, T. Becker, and E. M. Yeatman, "Design and fabrication of heat storage thermoelectric harvesting devices," *IEEE Transactions on Industrial Electronics*, vol. 61, no. 1, pp. 302–309, 2014.

[22] K. Nakagawa and T. Suzuki, "A high-efficiency thermoelectric module with phase change material for IoT power supply," *Procedia Engineering*, vol. 168, pp. 1630–1633, 2016.

[23] Z. Ma, Y. Wang, S. Wang, and Y. Yang, "Ocean thermal energy harvesting with phase change material for underwater glider," *Applied Energy*, vol. 178, pp. 557–566, 2016.

[24] A. Elefsiniotis, N. Kokorakis, T. Becker, and U. Schmid, "A novel high-temperature aircraft-specific energy harvester using PCMs and state of the art TEGs," *Materials Today: Proceedings*, vol. 2, no. 2, pp. 814–822, 2015.

[25] D. Samson, M. Kluge, T. Becker, and U. Schmid, "Wireless sensor node powered by aircraft specific thermoelectric energy harvesting," *Sensors and Actuators: A Physical*, vol. 172, no. 1, pp. 240–244, 2011.

[26] S. Ahmadi Atouei, A. Rezania, A. A. Ranjbar, and L. A. Rosendahl, "Protection and thermal management of thermoelectric generator system using phase change materials: an experimental investigation," *Energy*, vol. 156, pp. 311–318, 2018.

[27] C. B. Yu, S. H. Yang, S. Y. Pak, J. R. Youn, and Y. S. Song, "Graphene embedded form stable phase change materials for drawing the thermo-electric energy harvesting," *Energy Conversion and Management*, vol. 169, pp. 88–96, 2018.

[28] Y. Tu, W. Zhu, T. Lu, and Y. Deng, "A novel thermoelectric harvester based on high-performance phase change material for space application," *Applied Energy*, vol. 206, pp. 1194–1202, 2017.

[29] D. Liu, D. G. Yang, N. Yang, and P. Yang, "Study on the thermal conductivity of graphene/Si interface structure based on molecular dynamics," in *2016 17th International Conference on Electronic Packaging Technology (ICEPT)*, pp. 642–645, Wuhan, China, 2016.

[30] P. Ranut, E. Nobile, and L. Mancini, "High resolution microtomography-based CFD simulation of flow and heat transfer in aluminum metal foams," *Applied Thermal Engineering*, vol. 69, no. 1–2, pp. 230–240, 2014.